Design of a parallel plate shearing device for visualization of concentrated suspensions

Shakeel, Ahmad; van Kan, Paul J.M.; Chassagne, Claire

DOI
10.1016/j.measurement.2019.05.101

Publication date
2019

Document Version
Accepted author manuscript

Published in
Measurement: Journal of the International Measurement Confederation

Design of a Parallel Plate Shearing Device for Visualization of Concentrated Suspensions

Ahmad Shakeel,[1,3*] *Paul J. M. van Kan,*[2] *Claire Chassagne*[1]

[1] Faculty of Civil Engineering and Geosciences, Department of Hydraulic Engineering, Delft University of Technology, Stevinweg 1, 2628 CN Delft, The Netherlands

[2] Van Kan Scientific, Keucheniuspad 40, 6535 VR Nijmegen, The Netherlands

[3] Department of Chemical, Polymer & Composite Materials Engineering, University of Engineering & Technology, Lahore, KSK Campus, 54890 Pakistan

a.shakeel@tudelft.nl; vankanscientific@xs4all.nl; c.chassagne@tudelft.nl;

[*]**Corresponding author**

Ahmad Shakeel

Faculty of Civil Engineering and Geosciences, Department of Hydraulic Engineering, Delft University of Technology, Stevinweg 1, 2628 CN Delft, The Netherlands

Email: a.shakeel@tudelft.nl

Tel. +31(0)613091407

Abstract

A modified version of the commercially available RheOptiCAD® was developed to visualize the microscopic structural changes occurring in concentrated suspensions, such as the break-up of flocs in clay suspensions, under shearing action. This is made possible by replacing the inverted microscope used in the traditional RheOptiCAD set-up by an upright modular microscope equipped with a CMOS camera and epi-illumination. Our device retains the following features of the previous version of RheOptiCAD®: [i] uniaxial translational motion of two parallel plates, [ii] three modes of shear straining, [iii] controlled thermal environment, [iv] vacuum joining of microscopy glass slides. The validation of the new design was done using a model system of un-flocculated and flocculated kaolin suspensions and concentrated natural mud suspension. The results showed that the constructed device is a promising tool for studying, from fundamental and industrial perspectives, the microstructural behaviour of complex suspended systems under controlled thermal and mechanical conditions.

Keywords: Shearing cell, Strain-controlled, Optical microscope, Rheo-optics, Suspensions

1. Introduction

Complex systems, such as emulsions, colloidal suspensions, gels, polymeric and surfactant solutions, foams and pastes are commonly part of food and non-food products, consumed on daily basis. For these products, the study of their viscoelastic properties is key for industrial purposes. Shearing action combined with parameters like pressure, temperature, ageing time, ionic strength or pH can lead to structural changes in such complex systems. One of these changes is demixing or phase separation, driven by either gravitational gradient or thermodynamic forces. Optical rheometry, also known as rheo-optics, is a powerful technique to analyse the behaviour of these complex systems, as it allows the visualization of flow, deformation and restructuration of the system under shear. Combining standard rheological measurements with rheo-optics provides an understanding of rheological parameters such as yield strength, viscosity or thixotropy in relation with the observed structural changes.

With the progress in advanced microscopic techniques, many research groups have developed devices that combine microscopy and rheology [1-4]. The progress in optical shearing devices until 1998 has been summarized by Fuller [5] and Wagner [6] for 2D rheo-optics and 3D rheo-optics, respectively. Later, van der Linden et al. [7] presented the review of rheo-optical devices for food and non-food systems. The rheo-optic devices developed so far are based on either an optical device fitted to the commercial or existing shearing device, or alternatively a shearing system developed to combine with a commercial or existing optical device. The established accuracy of commercial rheometers led researchers to favour the development of optical techniques fitted to the existing rheometers [8]. However, these devices have some drawbacks, *e.g.* limited field-of-view and low magnification power. Custom-made shearing cells are very interesting alternatives due to the fine tuning and huge flexibility in the materials selection for the surfaces which come into contact with the sample, the possibility to analyse samples under larger deformations and the possibility to create a zero-velocity plane

77 (ZVP) at any position within the cell gap by having top and bottom plates moving in opposite
78 directions [9, 10].

79 Several optical techniques have been used in rheo-optical devices, depending on the material
80 under investigation and the observation scale. Different shearing devices like a 4-roll mill
81 [11], controlled strain rheometer [12], parallel plate [13, 14], and others [15] have been used
82 so far to perform deformation under controlled environment. Table 1 summarizes some
83 important details about the already reported rheo-optical systems, in comparison to our
84 designed system.

85 Table 1: Key characteristics of some of the already reported rheo-optical systems

Rheometer/Shearing Cell	Microscope/Camera	Advantages	Limitations	Ref.
IR-200 Rheometer without transducer, Quartz Cone & Plate/Plate-plate geometry	Upright Optical microscope, CCD camera, halogen white lamp	Rotation can be reversed, mechanism for temperature control	Largest image size 640 x 480 pixels, not suitable at high shear rates	[16]
Custom made parallel plate shear cell	Inverted confocal scanning laser microscope	Higher accuracy from mechanical point of view	Lengthy process for sample preparation, requirement of pair of cassettes for every analysis, difficulty in reproducibility, absence of temperature control mechanism	[17]
1. Custom made parallel plate shear cell 2. Anton-Paar MCR 301 Rheometer, Cone & Plate/Plate-plate geometry	1. Upright microscope objective with CCD camera, LED backlight source 2. Inverted microscope objective with CCD camera	1. Allows to shear a very large surface of sample (~70 cm^2) 2. Measurement of stress	**1.** Control of gap variation between the plates was difficult, stress measurement was not possible, possible movement of only bottom plate, no mechanism for temperature control **2.** Not suitable for suspensions due to inverted microscope	[14]
Custom made parallel plate shear cell	Confocal scanning laser microscope, CCD camera	Temperature controlling mechanism	Fixed gap, movement of only one plate	[18]
Custom made cone & plate shear cell	Inverted confocal scanning laser microscope, green He–Ne laser	Movement of both plates, imaging of planes parallel as well as perpendicular to glass plate	Fixed positon of microscope objective in cell, variation in gap width caused by a slight wobbling of the glass plate, not suitable for higher shear rates, no temperature controlling mechanism	[9]
Stress-controlled Bohlin Gemini Rheometer, Cone & Plate geometry	Inverted confocal scanning laser microscope	A wide range of shear strain, up to 50% amplitude	Fixed positon of microscope objective in cell, no recording of images (absence of camera)	[19]
Linear parallel-plate shear cell	Inverted fast confocal microscope	Wall slip prevention by coating the slides with disordered layers of colloid, solvent trap to minimize evaporation	Possible movement of only top plate, no temperature controlling mechanism	[2, 20]
Custom made parallel plate shear cell	Inverted fast-scanning confocal microscope	Teflon sheets to minimize evaporation, synchronization of image acquisition and shearing	Possible movement of only bottom plate, image size 512 × 512 pixels	[21]

		action		
Custom made parallel plate shear cell	Inverted microscope, CCD camera	Roughened plates to minimize wall slip, movement of both plates	Image size 1024 x 1024 pixels, only oscillatory mode of shearing	[22-24]
Anton-Paar MCR 301 Rheometer, Cone & Plate geometry	Inverted confocal scanning laser microscope	Sandblasted plates to minimize wall slip, solvent trap to minimize evaporation	Image size 512 × 512 pixels, fixed gap width between cone and plate	[25]
Velocity-controlled Couette rheometer	Inverted fluorescent microscope, CCD camera	Allows to access local velocities up to 1 m/s	Not suitable for suspensions due to inverted microscope	[3]
Stress-controlled rheometer AR2000, Cone & Plate/Plate-plate geometry	Inverted confocal scanning laser microscope	Roughened plates to minimize wall slip, solvent trap to minimize evaporation	Not suitable for suspensions due to inverted microscope	[8, 26]
Custom made parallel plate shear cell	Inverted confocal scanning laser microscope	Temperature controlling mechanism, vacuum joining of glass coverslip with the plate, movement of both plates	No stress measurement, not suitable for suspensions due to inverted microscope	[10, 27]
Custom built constant stress shear cell, Cone & Plate geometry	Inverted fast-scanning confocal microscope	Solvent trap to minimize evaporation, cost-effective, availability of range and resolution of applied stresses through selection of transfer fluid	Absence of temperature controlling mechanism, not suitable for suspensions due to inverted microscope	[28]
Custom made parallel plate shear cell	Inverted confocal scanning laser microscope	Stress measurement, Solvent trap to minimize evaporation, possibility of biaxial shear experiments	Absence of temperature controlling mechanism, gluing of cover slip with the plate, not suitable for suspensions due to inverted microscope	[4]
Anton-Paar MCR 301 Rheometer, Cone & Plate/Plate-plate geometry	Inverted laser scanning confocal microscope	Wide range of applied torque, presence of normal force sensor	Not suitable for suspensions due to inverted microscope, image size 256 × 256 pixels	[29]
Rotational rheometer HAAKE MARS III, Cone & Plate/Plate-plate geometry	Inverted polarized reflected light microscope, CCD camera	Temperature controlling mechanism, in addition to light microscopy RAMAN spectroscopy measurements also available	Not suitable for suspensions due to inverted microscope setup	[30]
Custom made parallel plate shear cell	Upright optical microscope, CCD camera	Temperature controlling mechanism	Possible movement of only bottom plate, suitable for small amplitude deformation	[31-33]
Custom made parallel plate shear cell	Upright optical microscope, CMOS camera, LED light	Suitable for suspensions due to upright microscope, temperature controlling mechanism, vacuum joining of glass coverslip with the plate, movement of both plates, gap variation between two plates is possible from 0-5 mm, CMOS camera instead of CCD which provides reduced blooming and smearing, image size 2592 x 2048 pixels with square pixels for undistorted image, fluorescent marker is not required, microscope objective with large working distance	No mechanism for stress measurement	This study

Many rheo-optical devices developed so far are laboratory models and only some of them have been commercialized. The Cambridge Shearing System [31] produced by Linkam Scientific Instrument Ltd. is the first commercialized system for optical analysis under rotational shearing action. A confocal rheo-scope, combination of confocal microscope and rheometer, has also been reported by Besseling et al. [8] which possessed rotational shearing

mode. However, the size, weight (greater than 10 kg) and cost of this device seem to have posed serious issues for its commercialization. The benefit of rotational motion over translation is the generation of an infinite shear and deformation. However, using rotational mode has the technical drawback of a compromised field of vision since the axis of motor rotation comes in line with the axis of observation through microscope objective. Use of translational motion overcomes this disadvantage because the axis of observation is at a right angle to the axis of motion during shearing action between *e.g.* parallel plates [10]. Wu et al. [17] developed a laboratory prototype of shearing cell based on translation mode. It was adapted to the inverted commercial CLSM device and possessed high accuracy from mechanical point of view.

Recently, a novel parallel plate rheological device (RheOptiCAD®) was designed by CAD Instruments and reported by Boitte et al. [10]. With this device a video recording during shearing is obtained from which the structural changes in the samples can be studied (changes in floc size, etc.). The device has primarily been designed to be mounted on an inverted microscope. Even though it can be used to visualize readily opaque structures [9], the device is not suited to analyse the optical behaviour of very concentrated clay suspensions (our topic of interest) as it makes use of transmitted light. This is why we proceeded to design an alternative set-up that would enable the study of these type of suspensions.

In the remainder of the article, we present the modified version of RheOptiCAD® with microscope system suited to analyse the behaviour of complex systems, particularly suspensions, under temperature-controlled conditions by shearing parallel-plate geometry. The design and specifications of the selected components are detailed. The set-up has been validated thanks to the pilot experiments. These experiments are done using un-flocculated and flocculated model kaolin suspensions. Additional experiments done on natural mud samples are also presented.

2. Design Considerations

The setup of our rheo-optical device makes use of the RheOptiCAD®, a parallel plate shearing device, commercially available from CAD Instruments (Illiers Combray, France) and introduced in 2012 [10] that can easily be coupled to a microscope. In short, the RheOptiCAD® device has been designed to enable optical analysis under a linear shearing force. During the measurement, a strain is applied in continuous, step or oscillation mode and a video recording is obtained. The analysis can be done in a temperature-controlled environment. The position of the shear plane in the cell can be adjusted by varying the velocity of the top and bottom plates.

Depending on the microscope used, an application-specific set-up involving the RheOptiCAD® and this microscope must be designed. In previous applications, the subject of study often was a heavily textured colloidal system like dough [10, 27], with high viscosity and being opaque. Therefore, the RheOptiCAD® device was used with an inverted confocal laser scanning microscope and fluorescent markers were used to visualize the changes in dough structure. Our aim is to study concentrated colloidal suspensions under shear accounting for the following constraints:

- The visualization of concentrated (very opaque) colloidal suspensions require the use of an upright microscope with an epi-illumination.
- Even in the presence of a sedimentation layer, the sample thickness should be much larger than the size of coagulated clay particles (0.1 mm). Therefore, microscope objectives with a large working distance (W. D.) should be selected. A simultaneous design constraint is that the objectives must have an (adjustable) cover slip correction.

- To study clay particles with their "native" charge, addition of fluorescent marker molecules is unwanted. Therefore, the microscope should operate with direct illumination.

In the following sections we present a complete functional design and technical implementation, which enables this new application of the RheOptiCAD® system.

3. Functional Design

3.1. Modification of the RheOptiCAD®

The RheOptiCAD® is manufactured by CAD Instruments (Illiers-Combray, France). The instrument is a modular design, contained in a cube-shaped frame with dimensions of about 20 x 20 x 20 cm and total weight of about 5 kg. The construction is designed for optimal stiffness, which is achieved by using an aluminium construction with rounded corners and a minimal number of bolted joints (Fig. 1). The device can be (re)positioned in a microscopic setup by means of the "handles" that form the device's skeleton. This leaves the relative positioning of the internal parts unchanged. Within the cube-shaped frame, three motorized linear-stages are mounted. These stages can move under closed-loop control and are computer-controlled. Furthermore, the temperature of the device can be actively controlled by a Peltier cooler in the bottom plate, (green in Fig. 1) which is also under computer control.

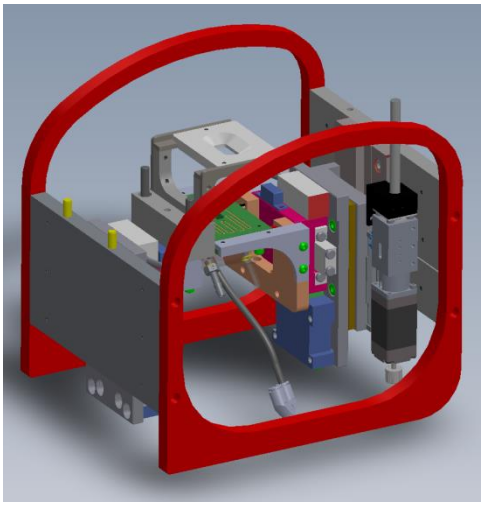

FIG. 1. 3D image of the RheOptiCAD® rheometric device, modified for observation from above. The microscope objective is lowered into the recessed area on the top plate for observation of particles in the sample cell between top and bottom plate.

The design of the top and bottom plate of the RheOptiCAD® was adapted for observation from above. An opening with an oval shape was made in the top plate, to accommodate the microscope objectives (18 mm x 8 mm = 144 mm^2), defining the dimensions of the observation window. Also, the vacuum ports in the top plate, necessary for the suction that keeps the glass slide in position, were moved to the side. In this way, sufficient horizontal and free vertical movement of the objectives was achieved. In the design presented here, with an upright microscope using epi-illumination and observation of reflected light, the displacement of the top plate is limited: the top plate can move with an amplitude of 12 mm, the bottom plate can travel as far as 20 mm.

3.2. Microscopy subsystem

For the upright microscope in the setup, we have found suitable components in the Olympus BXFM-BX3M modular microscopy/illuminator system [34]. From this modular system we have chosen the following parts:

- BX-FM-F Focusing unit, 30 mm range, 2 µm resolution
- Märzhäuser MFD motorised Z-stage drive mounted on the fine focusing knob[35]
- BX3M-KMA-S Epi-illuminator with white LED source
- U-5RE-2 5-fold nosepiece, equipped with:
    - LUCPLFLN 20x objective, coverslip correction (CC) 0-2 mm, W. D. 6.6-7.8 mm, NA 0.45
    - LUCPLFLN 40x objective, coverslip correction (CC) 0-2 mm, W. D. 2.7-4.0 mm, NA 0.6

- U-TLU-2 Telan lens-unit (tube lens)
- U-TV1X-2-7 1x video-adapter
- U-CMAD3-1-7 C-mount adapter ring

An impression of the microscopy subsystem is given in Fig. 2.

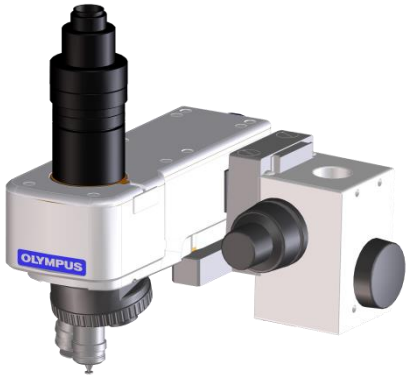

FIG. 2. The Olympus BXFM modular microscope with focusing unit (courtesy of Olympus). This microscope uses an LED white light source for broadband epi-illumination. Observation of the image in reflected light is done with a CMOS camera on top of the setup (not shown)

3.3. System assembly

The RheOptiCAD® skeleton and the microscope subsystem were assembled on a solid aluminium baseplate with adjustable feet for levelling. The focusing unit was attached to a solid stainless-steel rod with a diameter of 32 mm, according to Olympus factory specifications. The height was adjusted and fixed with an aluminium locking plate with six M6 Allen bolts (Fig. 3).

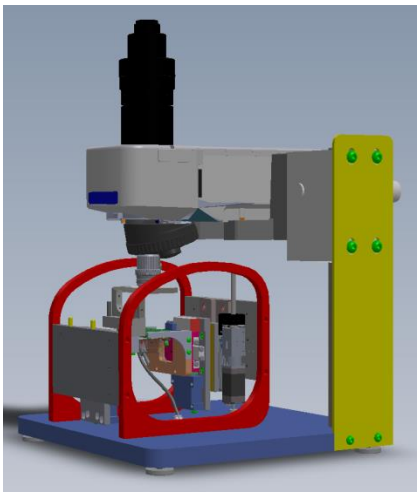

FIG. 3. The assembled modified RheOptiCAD® setup.

3.4. Mechanical Control

In the RheOptiCAD® device, the shearing of the sample is carried out by uniaxial translation, generated by the motion of two parallel (top and bottom) plates. Each plate is driven by its own linear stage (Nanomotion FB-075 with HR4 piezo-electric motor) (NanoMotion, USA)[36]. The translational mode of shearing enables to make use of the rectangular shape of commercial microscopy glass slides, which makes the sampling user friendly. A vertical translation with a third motorized stage enables easy separation of the top and bottom plates for sample loading (Fig. 4). The sample is placed on a rectangular microscopy cover slip (24 x 60 mm) attached to the bottom plate.

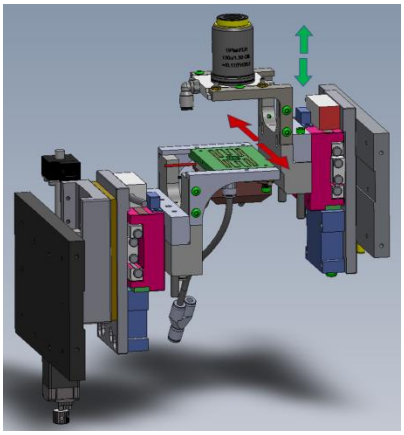

FIG. 4. Shear movement of the top and bottom plates of the RheOptiCAD® device (red arrows). Vertical movement of the bottom plate assembly enables loading of a suspension droplet on the bottom plate as well as adjustment of the cell height (green arrows)

To ensure the parallelism and planarity of microscopy glass slides, important for better observation and fine-tune controlling of deformation, the glass slides were bound to the aluminium plates (top and bottom) by creating vacuum between them. A path for air was imprinted on the surface of both plates and the output point was connected to the vacuum pump (LaboPort KNF, France) having a minimum pressure limit of 160 mbar [10].

Before measurement, the bottom plate is raised until the sample is in contact with both plates. Subsequently, the distance between the plates (gap width) is adjusted to the desired value, thereby enclosing the droplet. All axes of translation are motorized with closed-loop control. The absolute encoders, Renishaw (RGH24Y15D30A), with 10 nm resolution used for the horizontal translations retain their position information. The vertical encoder is recalibrated in the RheOptiCAD® software when the top and bottom glass cover slips are replaced [10]. The motor control and recording of the plate's position are done by a modular motor control device, (Galil DMC 4040 [37]), which also generates a trigger pulse to start camera image acquisition.

Focusing of the objective is performed by the stepper motor in the Märzhäuser MFD motorised Z-stage drive [35]. Manual handling of the focusing knob is replaced by control from the computer user interface. At start-up, the focusing unit is driven to its top position, indicated by a micro switch. In this way, the focusing unit is calibrated.

3.5. Optical image acquisition

The optical layout of the microscope system is presented in Fig. 5. The LED source, at the back of the setup, provides white light. The source is imaged at the back focal plane of the objective (Köhler illumination). The light is focused on the sample by the objective.

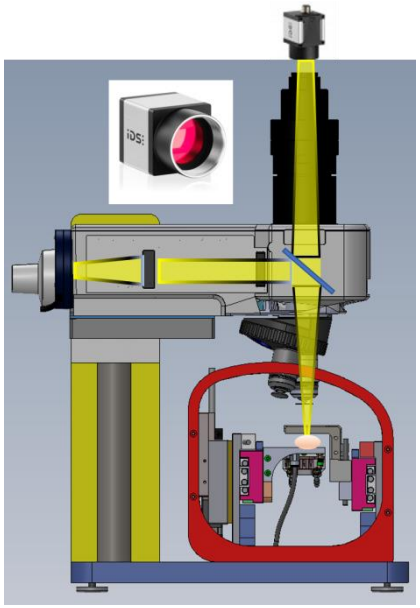

FIG. 5. The optical layout of modified RheOptiCAD® device. A 1" CMOS camera (see insert) is fitted on the epi-illumination module of the microscope.

We have chosen plan-fluorite objectives for this assembly, for the following reasons:

- planarity of the field of view is essential
- colour correction as provided by plan-apochromatic lenses is not necessary for our experiments. We want to observe, locate and track particles under shear; therefore, we use a monochrome camera for optimal resolution.
- availability and affordability of long-working distance objectives with cover slip correction

The objectives mentioned above provide a working distance which is suitable for the 0-5 mm gap width of the RheOptiCAD®. Furthermore, the coverslip correction ring enables improvement of the image of particles near the bottom of the sample.

The objective collects the reflected light from a horizontal slice in the sample. With the infinity-corrected optics chosen for this setup, a sharp image is created by a tube lens between the semi-transparent mirror and the camera. The focal length of this tube lens determines the image size on the camera. The Olympus tube lens and C-mount adapter for a 1" digital camera was chosen.

The camera selected was a USB 3.0 connected monochrome CMOS camera with a 1" target (12.5 x 10 mm) and a resolution of 2592 x 2048 pixels (UI-3180CP-M-GL Rev.2, IDS GmbH, D). This camera is based on a PYTHON5000 CMOS-chip (ON Semiconductor) [38] with some interesting features for microscopy:

- square 4.8 µm x 4.8 µm pixels for undistorted images
- a global shutter with various external trigger options via the control connector, this enables synchronization with the motion of the RheOptiCAD® plates.
- choice of a Reduced Area-of Interest (ROI) and increased framerate. This opens the option of using the camera at a resolution of 2048 x 2048 pixels, matching the circular (flat) field of view of the microscope. Depending on the USB connection, framerates of more than 80 Hz can be achieved.
- a CMOS sensor, apart from high resolution and high frame rate, provides reduced blooming and smearing compared to CCD devices. This is an advantage in particle tracking and analysis. Table 2 compares the features of the previous and current versions of the RheOptiCAD.

Table 2: Differences between the two versions of the RheOptiCAD systems

Component name	RheOptiCAD® [8]	Our device
Modular upright microscope		X
Inverted microscope	X	

CMOS camera with square pixels and reduced blooming and smearing		X
CCD camera	X	
Epi-illumination		X
Vacuum joining of glass slides	X	X
Peltier system for temperature control	X	X

3.6. Zero velocity plane

To analyse the structural changes in the sample under shear within the observation window, it is essential for the object to be in the zero-velocity plane (ZVP). The position of this ZVP between the plates in z-axis can be changed just by playing with the velocities of top and bottom plates (see Fig. 6), according to the following equation:

$$z_0 = \frac{e}{\frac{v_2}{v_1}+1} \quad (3)$$

with z_0 being the position of the ZVP in the z-axis direction, with the origin just underneath the top plate. v_1 and v_2, respectively, the velocities of the top and bottom plates (mm s^{-1}), and e the gap width (mm).

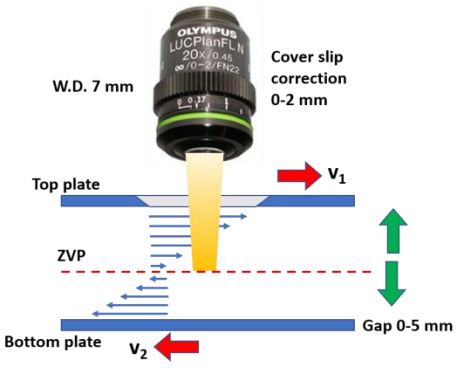

FIG. 6. Movement of top and bottom plates along x-axis to change the location of ZVP (red arrows). Green arrows represent the vertical movement (z-axis) of bottom plate for loading the sample and height adjustment

3.7. Temperature control

Temperature could be controlled within the range of 10-80^{o}C using a Peltier system TEC-1090 Controller/Peltier Driver (Meerstetter Engineering, CH) (30 mm × 30 mm) mounted on the bottom plate. Water circulation, in the copper part of Peltier system, was used to regulate the sample temperature and a thermistor was fitted to the aluminium body of the bottom plate to monitor the temperature. Heating and cooling rates were optimized within the range of 1-20^{o}C min^{-1} using the PID controller.

3.8. Control software

To make a user-friendly shearing device, a software was developed by CAD instruments, comprising of graphic interface, to define and control all the parameters related to the plates like, position of plates, mode of shear strain, velocity, amplitude, experiment time, frequency and gap width. Three modes of shear strain, after positioning the sample and setting the gap width, are available:

1. Step-strain for sudden deformation by having amplitude of each plate as variable (both plates are mobile)
2. continuous strain for linear deformation by having amplitude of each plate and experimental time as variables (both plates are mobile)
3. oscillatory strain for sinusoidal deformation by having amplitude and frequency of one of the plates as variable (one plate is mobile)

After each experiment, a data file is designed to be created automatically, which consists of the data supplied by the encoders of motorized stages. Different variables like position, time and velocity of top plate, bottom plate and gap width are recorded. Galil DMC-4040 acquisition system allows the recording of data points. Fig. 7 shows the scheme of complete

software configuration and Fig. 8 shows the developed shear cell with an upright optical microscope.

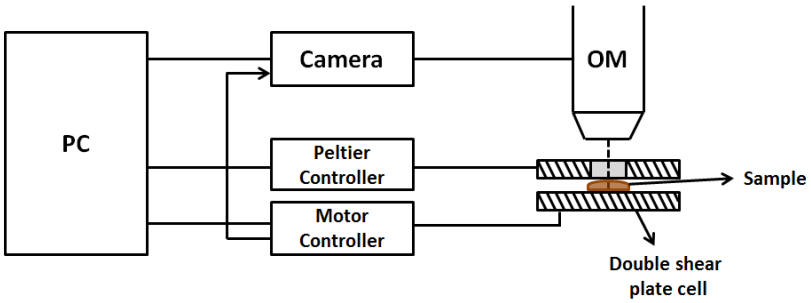

FIG. 7. Schematic representation of complete software configuration; PC = personal computer; OM = optical microscope. The motor controller triggers continuous camera acquisition when the shear motion starts.

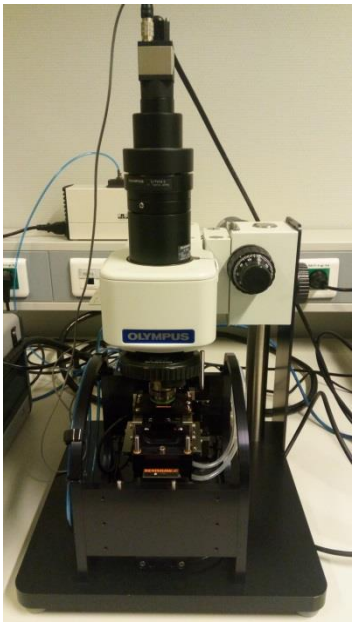

FIG. 8. Shear cell combined with an upright optical microscope and a camera

4. Validation Experiments

4.1. Kaolin suspension

The validation of the new set-up was performed with kaolin suspensions in water. Un-flocculated kaolin suspensions were prepared by dispersing small amount of kaolin (Imerys, England) in distilled water. Two commercial polyelectrolytes, Zetag 4120 (anionic copolymer of acrylamide and acrylic acid) and Zetag 8125 (cationic copolymer of acrylamide and quaternized ammonium cationic monomer) were used to prepare flocculated kaolin suspensions, by simply dispersing small amounts of polyelectrolytes and kaolin in distilled

water. For the optical analysis, we used our new optical microscope equipped with the 20x objective, having 0.45 NA and 6.6-7.8 mm of working distance. The gap between the two plates was varied from 100 to 10 μm for different samples. In all cases, the sample was in contact with both upper and lower plates. This ensures that the samples were deformed instead of displaced. The temperature was maintained at 20^{o}C for all the investigations. The LED light source was used and the images (2592 x 2048 pixels) were recorded in the x-y plane.

Several investigations were performed in oscillation mode using frequencies f between 0.5 and 2 Hz and amplitudes A ranging from 0.1 to 0.5 mm for the bottom plate. The value of the amplitude was carefully chosen to make sure that the particles remain in the frame of view during the whole experiment. Fig. 9 shows the snapshots from the video recording for the un-flocculated kaolin suspension. It can be easily seen from the images that the unmodified kaolin particles are very small and homogeneously dispersed within the water. Under oscillatory shear, the particles showed a little bit movement due to the absence of any interactions between the particles.

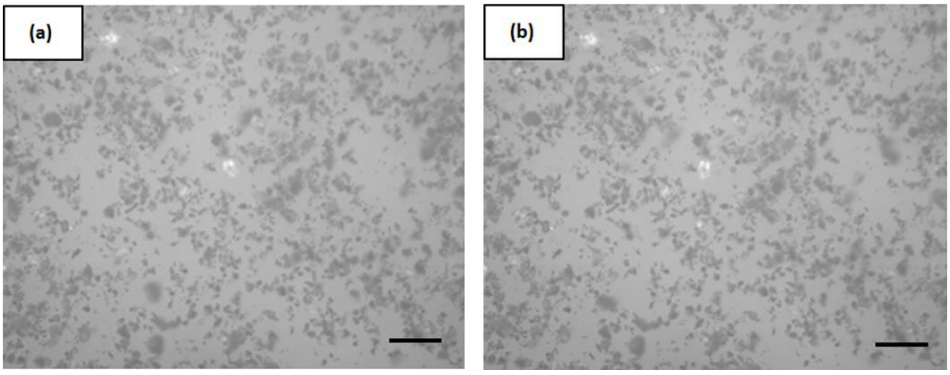

FIG. 9. Images of un-flocculated kaolin suspensions subjected to oscillation at (a) t = 0 s (b) t = 5 s; Gap width = 10 μm; f = 0.5 Hz; A = 0.1 mm. Slight movement of clay particles can be seen due to absence of interactions. Scale bar represents 70 μm

Figs. 10 and 11 present the images of the kaolin suspensions containing polyelectrolytes. All these images corroborate the formation of flocculated structures by addition of polyelectrolytes. Fig. 10 displays the break-up of a flocculated structure by the application of

a oscillatory shear for kaolin particles coated with cationic polyelectrolyte. Fig. 11b shows the stretching of a flocculated structure made of kaolin and anionic polyelectrolyte after 5 s of oscillatory shear at an amplitude of 0.5 mm and a frequency of 2 Hz.

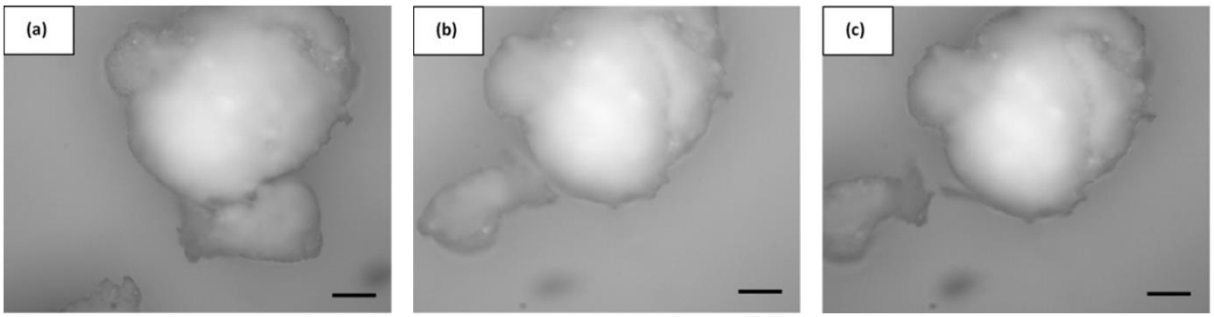

FIG. 10. Images of cationic polyelectrolyte-based kaolin suspensions subjected to oscillation at (a) t = 0 s (b) t = 3 s (c) t = 5 s; Gap width = 100 μm; f = 1 Hz; A = 0.4 mm. Sequence of images shows the break-up of flocs. Scale bar represents 70 μm

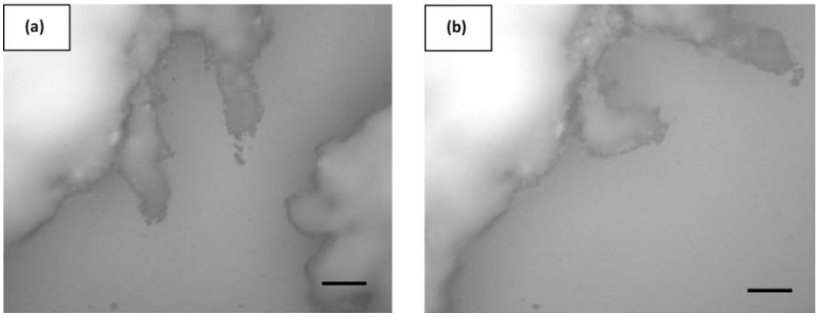

FIG. 11. Images of anionic polyelectrolyte-based kaolin suspensions subjected to oscillation at (a) t = 0 s (b) t = 5 s; Gap width = 100 μm; f = 2 Hz; A = 0.5 mm. Second image presents the stretching of flocs after 5 s. Scale bar represents 70 μm

4.2. Natural mud sample

A natural mud sample, collected from Port of Hamburg (Germany), was chosen for the investigation. The natural mud samples were placed on the bottom plate of the device and a gap of 100 μm was set to perform the experiments at 20^{o}C. Firstly, the samples were subjected to continuous strain by setting the movement of both plates in opposite directions. The images selected from the video recording (which can be found in the online supplementary material) are shown in Fig. 12. Fig. 12b shows the breakage/separation of a bigger flocculated structure into two flocs which further divided into more smaller flocs as shown in Fig. 12c.

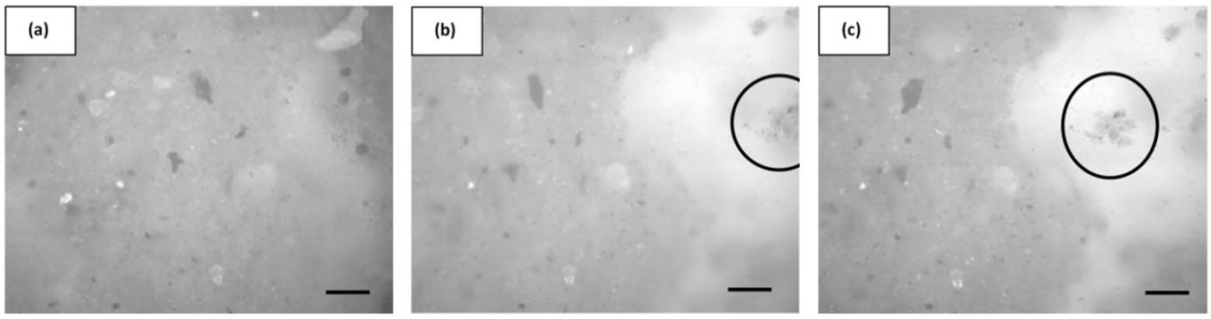

FIG. 12. Images of a natural mud suspension subjected to continuous strain at (a) t = 0 s, (b) t = 5 s, (c) t = 10 s. Sequence of images shows the structural break-up during shear. The black circle shows a small floc that has detached from a bigger one on the right (not in view). Scale bar represents 70 µm

The optical shearing of the samples was also performed in oscillation mode by oscillating the bottom plate at 1 Hz with the amplitude of 0.4 mm. The images selected from the video recording are shown in Figs. 13 and 14. Fig. 13b shows the breakage of a flocculated structure after 3 s of oscillation motion. Fig. 14a shows the presence of a large particle (clay) in the suspension, which displayed the rotational motion during oscillatory shearing as indicated by the arrows in Fig. 14b. This large particle also creates a void during oscillation after 10 s, as shown in Fig. 14c.

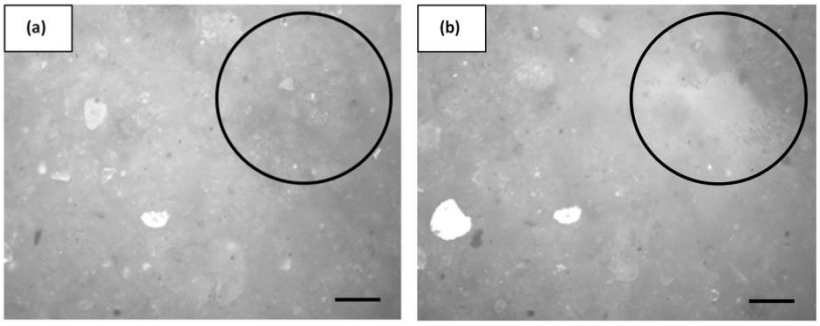

FIG.13. Images of a natural mud suspension subjected to oscillation at (a) t = 0 s, (b) t = 3 s. The black circle shows the result of the breakage of bigger flocs by the presence of a void (white colour) in the second image. Scale bar represents 70 µm

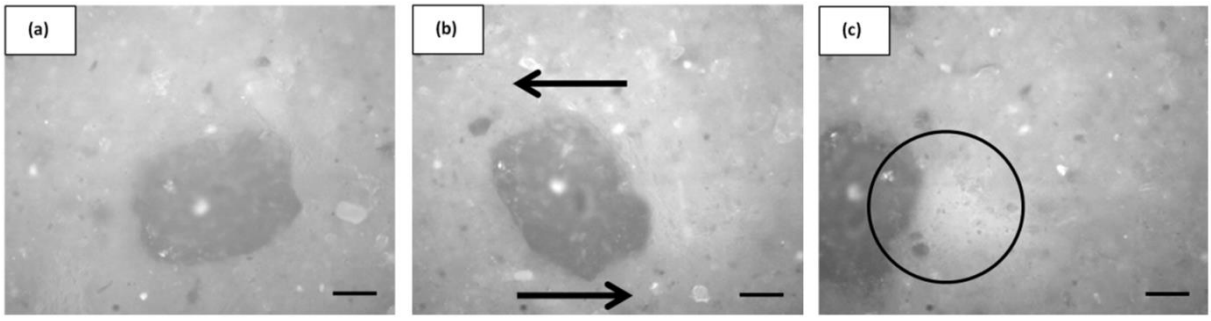

FIG. 14. Images of a natural mud suspension subjected to oscillation at (a) t = 0 s, (b) t = 5 s, (c) t = 10 s. Arrows shows the direction of rotational motion of particle during shearing. The white area inside the black circle represents a void created by the tumbling motion of the large particle. Scale bar represents 70 μm

5. Conclusion

This study presents the modification of an already reported rheo-optical device[10]. The modified system enables the observation of sedimentating and/or concentrated suspensions, by using an upright optical microscope configuration instead of an inverted one as in the original device. An optical microscope with epi-illumination using reflected light was used to get the optical signature of suspensions. Proof-of-concept experiments performed by using un-flocculated and flocculated kaolin suspensions and a natural mud suspension, confirmed the applicability of our device for investigating complex systems. Successive snapshots taken from the video recording of these suspensions under shear revealed the structural changes of these systems as a function of the shearing action. The new rheo-optical device will be used, in the future, to perform state of the art research in the field of sediment rheology by linking the qualitative structural break-up and build-up (thixotropy) of mud suspensions observed by the present device to the quantitative rheological measurements obtained from a conventional rheometer.

In future applications/research, some technical modifications can be done to optimize the presented device such as: [i] incorporating a device for stress measurement (material's response to the applied deformation), [ii] having a translation motion of plates in y-axis, in addition to x-axis, [iii] adding the possibility to have oscillation of both plates simultaneously, instead of one plate, in oscillation mode, [iv] modifying the surface properties of the glass slides in case of sticky materials which would also enable to study particle-wall interactions, and [5] improving the data analysis software for quantitative investigation.

Acknowledgements

399 The authors would like to thank CAD Instruments, France, in particular Claude Vizcaino, and
400 Olympus, The Netherlands particularly Ronald van Dijk, for their technical contribution. This
401 study was partially supported by funding from the Netherlands Organization for Scientific
402 Research (NWO), project no. 850.13.031.

References

[1] P. Schall, D.A. Weitz, F. Spaepen, Structural Rearrangements That Govern Flow in Colloidal Glasses, Science, 318 (2007) 1895-1899.

[2] N. Koumakis, M. Laurati, S.U. Egelhaaf, J.F. Brady, G. Petekidis, Yielding of Hard-Sphere Glasses during Start-Up Shear, Phys. Rev. Lett., 108 (2012) 098303.

[3] J. Goyon, A. Colin, G. Ovarlez, A. Ajdari, L. Bocquet, Spatial cooperativity in soft glassy flows, Nature, 454 (2008) 84-87.

[4] N.Y.C. Lin, J.H. McCoy, X. Cheng, B. Leahy, J.N. Israelachvili, I. Cohen, A multi-axis confocal rheoscope for studying shear flow of structured fluids, Rev. Sci. Instrum., 85 (2014) 033905.

[5] G.G. Fuller, Optical rheometry of complex fluid interfaces, Current Opinion in Colloid & Interface Science, 2 (1997) 153-157.

[6] N.J. Wagner, Rheo-optics, Current Opinion in Colloid & Interface Science, 3 (1998) 391-400.

[7] E. van der Linden, L. Sagis, P. Venema, Rheo-optics and food systems, Current Opinion in Colloid & Interface Science, 8 (2003) 349-358.

[8] R. Besseling, L. Isa, E.R. Weeks, W.C.K. Poon, Quantitative imaging of colloidal flows, Adv. Colloid Interface Sci., 146 (2009) 1-17.

[9] D. Didi, W. Hans, B. Alfons van, I. Arnout, Confocal microscopy of colloidal dispersions in shear flow using a counter-rotating cone–plate shear cell, J. Phys.: Condens. Matter, 16 (2004) S3917-S3927.

[10] J.-B. Boitte, C. Vizcaïno, L. Benyahia, J.-M. Herry, C. Michon, M. Hayert, A novel rheo-optical device for studying complex fluids in a double shear plate geometry, Rev. Sci. Instrum., 84 (2013) 013709.

[11] L. Hamberg, P. Walkenström, M. Stading, A.-M. Hermansson, Aggregation, viscosity measurements and direct observation of protein coated latex particles under shear, Food Hydrocolloids, 15 (2001) 139-151.

[12] F. Mighri, M.A. Huneault, Dispersion visualization of model fluids in a transparent Couette flow cell, J. Rheol., 45 (2001) 783-797.

[13] Y. Deyrail, P. Cassagnau, Phase deformation under shear in an immiscible polymer blend: Influence of strong permanent elastic properties, J. Rheol., 48 (2004) 505-524.

[14] V. Grenard, N. Taberlet, S. Manneville, Shear-induced structuration of confined carbon black gels: steady-state features of vorticity-aligned flocs, Soft Matter, 7 (2011) 3920-3928.

[15] B. Noetinger, L. Petit, E. Guazzelli, M. Clément, Réalisation d'une cellule à cisaillement elliptique, Rev. Phys. Appl. (Paris), 22 (1987) 1025-1032.

[16] T. Kume, K. Asakawa, E. Moses, K. Matsuzaka, T. Hashimoto, A new apparatus for simultaneous observation of optical microscopy and small-angle light scattering measurements of polymers under shear flow, Acta Polym., 46 (1995) 79-85.

[17] Y.L. Wu, J.H.J. Brand, J.L.A.v. Gemert, J. Verkerk, H. Wisman, A.v. Blaaderen, A. Imhof, A new parallel plate shear cell for in situ real-space measurements of complex fluids under shear flow, Rev. Sci. Instrum., 78 (2007) 103902.

[18] E. Tamborini, L. Cipelletti, L. Ramos, Plasticity of a Colloidal Polycrystal under Cyclic Shear, Phys. Rev. Lett., 113 (2014) 078301.

[19] A. Basu, Q. Wen, X. Mao, T.C. Lubensky, P.A. Janmey, A.G. Yodh, Nonaffine Displacements in Flexible Polymer Networks, Macromolecules, 44 (2011) 1671-1679.

[20] R. Besseling, E.R. Weeks, A.B. Schofield, W.C.K. Poon, Three-Dimensional Imaging of Colloidal Glasses under Steady Shear, Phys. Rev. Lett., 99 (2007) 028301.

[21] J. Zausch, J. Horbach, M. Laurati, S.U. Egelhaaf, J.M. Brader, V. Th, M. Fuchs, From equilibrium to steady state: the transient dynamics of colloidal liquids under shear, J. Phys.: Condens. Matter, 20 (2008) 404210.

[22] E.D. Knowlton, D.J. Pine, L. Cipelletti, A microscopic view of the yielding transition in concentrated emulsions, Soft Matter, 10 (2014) 6931-6940.

[23] G. Petekidis, A. Moussaïd, P.N. Pusey, Rearrangements in hard-sphere glasses under oscillatory shear strain, Physical Review E, 66 (2002) 051402.
[24] D. Chen, D. Semwogerere, J. Sato, V. Breedveld, E.R. Weeks, Microscopic structural relaxation in a sheared supercooled colloidal liquid, Physical Review E, 81 (2010) 011403.
[25] T. Sentjabrskaja, P. Chaudhuri, M. Hermes, W.C.K. Poon, J. Horbach, S.U. Egelhaaf, M. Laurati, Creep and flow of glasses: strain response linked to the spatial distribution of dynamical heterogeneities, Scientific Reports, 5 (2015) 11884.
[26] R. Besseling, L. Isa, P. Ballesta, G. Petekidis, M.E. Cates, W.C.K. Poon, Shear Banding and Flow-Concentration Coupling in Colloidal Glasses, Phys. Rev. Lett., 105 (2010) 268301.
[27] J.B. Boitte, M. Hayert, C. Michon, Observation of wheat flour doughs under mechanical treatment using confocal microscopy and classification of their microstructures, Journal of Cereal Science, 58 (2013) 365-371.
[28] H.K. Chan, A. Mohraz, A simple shear cell for the direct visualization of step-stress deformation in soft materials, Rheol. Acta, 52 (2013) 383-394.
[29] S.K. Dutta, A. Mbi, R.C. Arevalo, D.L. Blair, Development of a confocal rheometer for soft and biological materials, Rev. Sci. Instrum., 84 (2013) 063702.
[30] A.P. Kotula, M.W. Meyer, F. De Vito, J. Plog, A.R.H. Walker, K.B. Migler, The rheo-Raman microscope: Simultaneous chemical, conformational, mechanical, and microstructural measures of soft materials, Rev. Sci. Instrum., 87 (2016) 105105.
[31] S. Wannaborworn, M.R. Mackley, Y. Renardy, Experimental observation and matching numerical simulation for the deformation and breakup of immiscible drops in oscillatory shear, J. Rheol., 46 (2002) 1279-1293.
[32] K. Tanaka, K. Yonetake, T. Masuko, R. Akiyama, Shearing microscopy using polarized optical microscope with shear stage and spectral analyser to study liquid crystalline polymers, Journal of Microscopy, 205 (2002) 15-20.
[33] M.R. Mackley, S. Wannaborworn, P. Gao, F. Zhao, The optical microscopy of sheared liquids using a newly developed optical stage, Microscopy and Analysis, 69 (1999) 25–27.
[34] https://www.olympus-ims.com/en/microscope/bxfm.
[35] https://www.marzhauser.com/nc/en/pim/productdetail/pimview/single/pimid/p60.html?filter=p50&cHash=083883ba4af55655852019fc9ee88051.
[36] http://www.nanomotion.com/motion-product/fb075-linear-stage.
[37] http://www.galilmc.com/motion-controllers/multi-axis/dmc-40x0.
[38] https://www.onsemi.com/pub/Collateral/NOIP1SN5000A-D.PDF.